PCCP

Accepted Manuscript

ROYAL SOCIETY OF CHEMISTRY

www.rsc.org/pccp

Adsorption–desorption oscillations of nanoparticles on honeycomb-patterned pH-responsive hydrogel surface were derived by a pH-oscillator in a closed reaction system

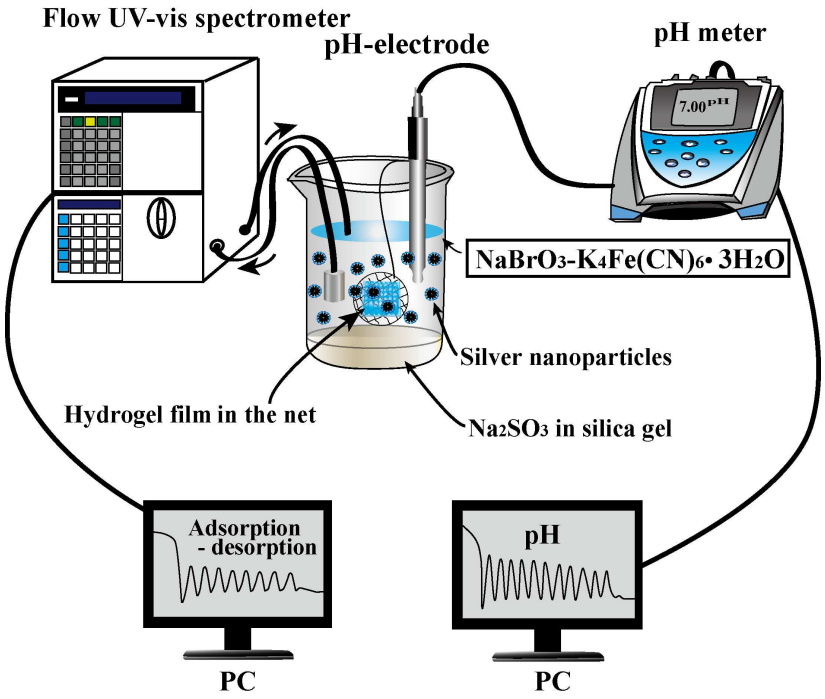

Adsorption–desorption oscillations of nanoparticles on honeycomb-patterned pH-responsive hydrogel surface in a closed reaction system

Ji Ho Jang,[a] M. Orbán,[b] Shutao Wang,[c] and Do Sung Huh[a*]

[*]Corresponding Author: Do Sung Huh

Email: chemhds@inje.ac.kr; Tel: 82-55-320-3225; Fax: 82-55-321-9718

A new type of pH-responsive hydrogel surface with varying nanoparticle adsorptivities was fabricated to a micro-patterned film. To increase responsivity to environmental pH changes, we incorporated graphene oxide (GO) into a poly(methacrylic acid)–polyethylene glycol copolymer. Incorporating GO in the pH-responsive hydrogel significantly increased the adsorption–desorption responsivity of Ag nanoparticles on the gel surface. A pH oscillator in a closed reaction system composed of BrO_3^-–$Fe(CN)_6^{4-}$–SO_3^{2-} facilitated the self-oscillating adsorption–desorption of Ag nanoparticles on the GO-incorporated gel surface. The reversible adsorption–desorption of Ag nanoparticles on the patterned hydrogel surface in response to pH oscillations was determined using UV–visible spectroscopy in aqueous solution. The observed heterogeneous oscillations indicated that the adsorptivity of the gel surface can be reversibly changed on the patterned pH-responsive gel. This phenomenon is similar to various natural biological systems.

Keywords: Composite hydrogel; Graphene oxide; pH oscillator; pH-responsive gel surface; Adsorption–desorption oscillation

1. Introduction

Living systems respond to external stimuli by adapting to changing conditions. Polymer scientists have endeavored to mimic such natural responses over the last 20 years by creating smart or intelligent polymers.[1,2] These polymers undergo reversible physical or chemical changes in response to external changes in environmental conditions, such as temperature,[3] pH,[4,5] light,[6] magnetic or electric field,[7] ionic strength,[8] and biological molecules.[9] Smart polymers have promising applications in the biomedical field as delivery systems for therapeutic agents, tissue-engineering scaffolds, cell culture supports, bioseparation devices, sensors, or actuator systems.[10–15]

The response mechanism of a polymer network is based on its chemical structure (including the functionality of side-chain groups, branches, crosslinks, and so on). Polymers that are sensitive to temperature changes are the most studied class of environmentally sensitive polymers because of their potential applications. This type of system exhibits a critical solution temperature (typically in water) at which the phases of polymer and solution change in accordance with their composition. The polymers sensitive to pH contain polyelectrolytes with weak acidic or basic group that accept or release protons in response to changes in environmental pH. Pendant acidic or basic groups on polyelectrolytes undergo ionization similar to the acidic or basic groups of

monoacids or monobases. Generating the charge along the polymer backbone causes the electrostatic repulsion to increase the hydrodynamic volume of the polymer.[16]

Stimuli-sensitive hydrogels have several potential applications; however, one of the major limitations of bulk hydrogels is their stolid volume change in response to environmental stimuli. Hence, a fast response to external stimuli is required for effective application of bulk hydrogels. Reducing bulk stimuli-sensitive hydrogel to small particles is a promising approach because the response rate is inversely proportional to the square of the characteristic dimension of the hydrogel.[17] Moreover, preparing nano- or micro-sized hydrogel particles is an important issue; therefore, stimuli-responsive hydrogels have been fabricated for potential applications in micro-actuators, micro-fluidics, drug delivery systems, tissue engineering, biosensors, and so on.[18–26]

In addition to reducing the hydrogel size for more effective applications, micro-fabricating smart hydrogels as patterned thin films is an effective method to increase their applicability. Stimuli-sensitive hydrogels fabricated into highly ordered nano- or micro-scale structures provide fast response to external stimuli and contain large surface area for immobilizing the released materials. Controlling such highly ordered structures with external stimuli could result in development of new functional materials, such as intelligent surface and tunable photonic materials.

Hydrogel films with ordered structure can be easily fabricated using highly ordered honeycomb-patterned porous films as a template through the method introduced by Pitois et al.[27] The fabrication of highly ordered gel materials using porous honeycomb-patterned polymer film as a template was firstly introduced by Yabu et al.[28-30] In addition, highly oriented nano-pit arrays are also obtained using shrinkable template, which can be used to change the shapes and sizes of honeycomb pores.[31]

However, the stimuli-responding behavior of responsive hydrogels is a temporary action toward an equilibrium state. For these systems, the on–off switching of external stimuli is essential to agitate the action of the hydrogels. The gels provide only one unique action, which could be swelling or shrinking, depending on the environmental condition of the switching. Moreover, autonomous oscillation, namely, spontaneous changes with temporal periodicity, such as heartbeat, brain waves, pulsatile secretion of hormone, cell cycle, and biorhythm, can be a characteristic behavior in living systems.

Several stimuli-responsive polymer systems that could self-oscillate without the on–off switching of external stimuli have been developed by Yoshida et al.[32] for biomimetics. A novel gel that provides mechanical oscillation by itself without external control in a complete closed solution was obtained. Self-oscillating hydrogels were acquired by incorporating an oscillating chemical reaction in a polymer network.

These scholars focused on the Belousov–Zhabotinsky (BZ) reaction, which is an oscillating reaction that exhibits temporal and spatiotemporal oscillating phenomena. The development of the self-oscillating hydrogels that utilize the BZ reaction is important in understanding biological phenomena, such as heartbeat and self-walking Mollusca.

Self-oscillating hydrogels based on pH-oscillatory system have been studied. pH-responsive hydrogels soaked in an autonomous pH-oscillating solution have been used to obtain periodic swelling–deswelling changes, whereas pH-sensitive gel membranes coupled with pH-oscillations or enzymatic reactions have been used to generate an oscillatory drug release system.[33] However, almost all pH oscillators function only under continuous flow stirred-tank reactor[34] or semi-batch reactor conditions;[35–37] in which all or some of the reagents are continuously supplied into the reactor to maintain the system away from the chemical equilibrium. Long-term large-amplitude pH oscillations are not feasibly obtained for the proposed application, which is a close reactor without continuous inflow of reagents. However, pH-oscillations in a closed system have recently been developed by Rabai[38] and Poros et al.[39] using batch reactor without continuous supply of any reagent into the reactor. Thus, self-oscillating hydrogels were developed by Wang et al.[40] and Bilici et al.[41] by utilizing the pH

oscillator in a closed system. Their studies also focused on the applications of self-oscillating gels induced by a pH-oscillator to generate mechanical energy for self-walking actuators and other devices.

In addition to the volume changes induced by mechanical energy from pH-responsive gels, adsorptivity on the hydrogel surface is accompanied by pH changes; the protonation degree of the acid group in the gel network alters the hydrophobic interaction on the hydrogel surface. As a universally weak interaction in nature, hydrophobic interaction changes water adsorption on smart hydrogel surfaces. Therefore, novel smart surfaces can be designed using hydrophobic interactions, which can change the adsorptivity of the surfaces of hydrogels to target materials. Therefore, hydrogel surface systems can be effectively applied to detect and sense specific target materials compared with bulk hydrogels. The application of bulk hydrogels in detection and sensing systems is restricted by its diffusion rate-limited transduction of signals.

Graphene oxide (GO) and GO-based nanocomposites have received significant attention because of their exceptional performance, including their conductive, mechanical, thermal, and biocompatible properties.[42–44] However, GO-incorporated pH-responsive composite hydrogels have been rarely reported.[45–48] The effect of GO on the reversible adsorption–desorption of target nanoparticles on composite hydrogel surface

has not been studied. At high pH, the –COOH groups of GO in hydrogels are fully charged; thus, GO is more hydrophilic and assists the release of adsorbed particles. However, as pH decreases, GO becomes protonated, less charged, and more amphiphilic, resulting in the adsorption of nanoparticles. GO surface has high specific surface area and abundant hydrophilic groups;[48–52] therefore, GO is a good candidate for fabricating novel self-oscillating pH-responsive hydrogels for the adsorption–desorption of nanoparticles or for specific materials with significantly increased applications.

In the present study, a novel composite pH-responsive gel incorporated with GO was fabricated to a highly ordered film to increase the sensitivity of the adsorption–desorption of nanoparticles. The composite hydrogel was prepared by incorporating GO into the copolymer grafted with poly(methacrylate)–polyethylene glycol (PMAA–PEG). Ag nanoparticles were used to determine the varying adsorption–desorption behavior on the hydrogel surface depending on the environmental pH. The adsorption–desorption sensitivity of the highly ordered GO-incorporated hydrogel film was compared with three types of similar hydrogel films: (1) GO was incorporated in an unordered film (which means a flat film); (2) Go was not incorporated in an ordered film; and (3) GO was not incorporated in an unordered film (which also means a flat film). In the ordered films, a patterned structure of the hydrogel surface that depends on the environmental

pH change was obtained. Scanning electron microscopy (SEM) was used to determine the effect of pH change on the patterned structure, which has an important role in the adsorptivity of hydrogel surfaces. For the reversible adsorption–desorption of nanoparticles on the GO-incorporated hydrogel surface, a pH-oscillatory reaction system (i.e., BrO_3^-–$Fe(CN)_6^{4-}$–SO_3^{2-}) in a closed condition was adopted.[39]

2. Experimental

2.1. Chemicals

The following chemicals were obtained from Sigma–Aldrich Korea (Seoul, Korea): polystyrene (PS, average MW = 400,000 g/mol), silver nitrate (99.9%), acetonitrile (99.8%), poly-N-vinylpyrrolidone (PVP, average MW = 40,000 g/mol), methacrylic acid (MAA), PEG methyl ether monomethacrylate (PEGMMA, average MW = 1,000 g/mol), tetraethylene glycol dimethacrylate (TEGDMA), 1-hydroxycyclohexyl phenyl ketone (Irgacure 184), sulfuric acid (99%), anhydrous sodium sulfite (99%), potassium hexacyanoferrate(II) trihydrate (98.5%), sodium bromate (99.8%), sodium silicate solution (approximately 27% SiO_2 and 14% NaOH), graphite (powder, with an average particle size of 6 μm), sodium nitrate (99%), potassium permanganate (99%), hydrogen peroxide aqueous solution (30%), hydrochloric acid (36.5%), sodium hydroxide (98%), and chloroacetic acid (99%). 6-Armed polyethylene glycol-amine was

purchased from Sunbio Inc., whereas tetrathiafulvalene (TTF) was purchased from John Mattey Co. All of the reagents were used as received without further purification. Deionized water was used in all of the experiments.

2.2. Procedures

2.2.1. Fabrication of GO-incorporated pH-responsive hydrogel surface changing in its morphology by pH variations

For the fabrication of GO-incorporated hydrogel with patterned surface, homogeneous soluble GO nanoparticles were chemically modified into an ethanol/water solution. Graphite powder was chemically oxidized using a modified Hummers method to obtain GO nanoparticles.[53] For the chemical modification of GO, the GO nanoparticles were treated with PEG. For PEGylation, 5 mL of the GO aqueous solution was diluted to obtain 2 mg/mL and then bath sonicated for 1 h to obtain a clear solution. NaOH (1.2 g) and chloroacetic acid (1.0 g) were added to 10 mL of the GO suspension (approximately 2 mg/mL) and bath sonicated for 1 h to 3 h to convert the –OH groups to –COOH by conjugating the acetic acid moieties. The obtained GO–COOH solution was neutralized and purified by rinsing and filtration. The GO–COOH suspension was diluted with water to obtain an optical density of 0.4 at 808 nm. 6-Armed PEG-amine

(2 mg/mL) was added into the GO–COOH suspension. The suspension was then sonicated for 5 min to obtain PEG–GO.[54]

For the fabrication of GO-incorporated hydrogel into the patterned surface, photo-polymerization using the honeycomb-patterned PS thin film as template was performed through the methods introduced in our previous report.[55] For the preparation of monomer solution, MAA (0.43 g, 0.05 M) and PEGMMA (2.50 g, 0.05 M) were dissolved in an ethanol/water solution (50:50 volume ratio). The crosslinking agent of TEGDMA (0.25 g) and the initiator 1-hydroxycyclohexyl phenyl ketone (Irgacure 184; 1.46 g) were added to the monomer solution with 0.75 mol% and 0.5 wt% total monomer, respectively. Subsequently, 0.8 mL of the PEG–GO solution was added to 4 mL of the monomer solution to obtain pre-gel solution. The Petri dish containing the PS template dish was placed in a vacuum chamber. Briefly, 4 mL of the pre-gel solution containing the monomer solution and PEG–GO was poured on the Petri dish to fabricate a convex-patterned hydrogel film. After removing air in the vacuum chamber using a vacuum pump for 1 min, the chamber was filled with nitrogen. The mold was then exposed to UV light (Hamamatsu Co. L8252A) for 5 min on the template. The patterned hydrogel film was prepared by peeling the film from the PS template and then rinsing with deionized water for several times. A pure-grafted copolymer hydrogel

containing MAA and PEGMMA without GO incorporation was also prepared using the same procedure. For comparison, flat films without patterns were also prepared through the same procedure but without using the honeycomb-patterned PS template. The overall experimental scheme for the preparation of the patterned GO-incorporated composite hydrogel film is shown in Figure 1.

To investigate the morphological changes of the patterned hydrogel surface in response to variations in environmental pH of the aqueous solution, we soaked the patterned hydrogel films in acidic and basic buffer solutions (pH 4 and 9, respectively). The convex-patterned gel films were equilibrated at a given pH condition and then investigated using SEM (COXEM CX-100s). The gels were immediately frozen by soaking in liquid nitrogen and then lyophilized for 24 h before SEM observation.

2.2.2. Adsorptivity and desorptivity of Ag nanoparticles on pH-responsive hydrogel surface

The reversible adsorption–desorption oscillations on the patterned GO-incorporated hydrogel surface were investigated. Adsorptivity and desorptivity of Ag nanoparticles on the four types of pH-responsive hydrogel surfaces were examined in pH 4 and 9 buffer solutions, respectively, to compare their adsorptions under different pH

conditions. Adsorptivity and desorptivity were determined using buffer solutions at a constant temperature of 45 °C. This temperature was set in our experiments when the reversible adsorption–desorption induced by the pH-oscillatory system was followed.

The hydrogels were separately soaked in the buffer solutions containing similar concentrations of Ag nanoparticles. The change in absorbance caused by the adsorption or desorption of Ag particles in the buffer solutions was determined using a flowing UV–vis detector (Hitachi L-7400). In addition, the adsorbed Ag particles on the hydrogel surfaces were also determined using SEM equipped with an energy-dispersive X-ray analyzer (EDS, Oxford instruments 7418). The Ag nanoparticles for the adsorption–desorption experiments were prepared by reducing $AgNO_3$ using TTF and PVP. TTF derivatives function as electron donors and then form stable charge-transfer complexes with various organic and inorganic acceptor species.[56] The procedure for Ag metallization was introduced in our previous report.[57]

2.2.3. Reversible adsorption–desorption oscillations of Ag nanoparticles on the GO-incorporated composite hydrogel surface

The oscillatory system comprising BrO_3^-–$Fe(CN)_6^{4-}$–SO_3^{2-} was used for pH oscillations in a closed chemical system to induce reversible changes of adsorption–

desorption on the GO-incorporated patterned hydrogel surface. Oscillations are not accompanied by color change, thus affecting the measurement of Ag concentration in the solution with a flowing UV-vis spectrometer. For the reaction system, stock solutions of bromate (0.6 M) and ferrocyanide (0.08 M) were prepared with distilled water from a Millipore purification system. The $K_4Fe(CN)_6$ stock solution was allowed to stand for 1 d and then stored in an amber glass bottle. For the preparation of the silica gel layer loaded with Na_2SO_3, 30.0 g of sodium silicate solution was diluted with approximately 70 mL of distilled water in a beaker. Anhydrous Na_2SO_3 (25.2 g) was dissolved in the solution (under gentle heating to accelerate the dissolution). The resulting mixture was transferred into a volumetric flask and filled to 100 mL using distilled water. This stock solution containing 2 M Na_2SO_3 was referred as "gel base" hereafter. Gelation was initiated by adding 2.5 cm^3 1 M H_2SO_4 to 7.0–7.5 cm^3 gel base in a 50 mL beaker, which was used as the reaction vessel for the closed-system experiments. Gelation was completed within 1–2 min. The beaker with the gel layer can be immediately used as the reactor for batch experiments. The pH oscillation reaction was performed at a constant temperature of 45 °C.

The oscillating pH was measured using a pH meter (Orion Multimeter Model No. 1219001). For the adsorption–desorption oscillations of Ag nanoparticles derived with

the pH-oscillation reaction, the patterned hydrogel film (1.5 cm × 1.5 cm × 1.0 mm) was placed into a net and then submerged into the oscillatory mixture. The oscillations of adsorption–desorption were detected using a flowing UV–vis detector at a constant flow rate of 2.0 mL/min. The experimental scheme for the simultaneous detection of pH and adsorption–desorption oscillations induced by the pH oscillator in the closed system is illustrated in Figure 2.

3. Results and Discussion

3.1. Hydrogel films with patterned surface and morphological structure change induced by environmental pH variations

Figures 3(a) and 3(b) show typical SEM images of the patterned hydrogel films with and without GO incorporation, respectively. In Figure 3(a), the left picture shows the surface image, the right picture represents the cross-sectional image, and the bottom part depicts the SEM–EDS analysis. The SEM images for the two patterned hydrogel films exhibited regularly ordered convex and hexagonal structures. This finding indicates that the experimental method used in this study was effective and facile for preparing micro-patterned hydrogel films. No significant difference was found in the obtained SEM image of the two hydrogel surfaces regardless of GO incorporation. However, the

SEM–EDS images of the two hydrogel films were significantly different. The peaks indicating C and O were significantly increased by the incorporation of GO, indicating that GO was incorporated in the PMAA–PEG hydrogel. Figure 3(c) shows a typical SEM image for the honeycomb-patterned PS film used as template in fabricating patterned hydrogel films.

Figure 4 shows typical SEM images of the patterned hydrogel surfaces altered by environmental pH variation. The images were obtained after the hydrogel film was soaked in buffer solutions at pH 4 and 9 for 10 min. For the SEM observation depending on the environmental pH, the gels were immediately frozen by soaking in liquid nitrogen and were lyophilized for 24 h.

The left and right pictures show typical images of the hydrogel films that were soaked in pH 4 and 9 buffer solutions for 10 min, respectively. The results show that the surface morphology of the hydrogel surface was sensitive to environmental pH variations. The highly ordered hexagonal patterns of the hydrogel films are shown in Figures 3(a) and 3(b), whereas the patterns altered by environmental pH are presented in in Figures 4(a) and 4(b). The structure of the patterns changed into a squeezed state compared with the original structure after soaking in the buffer solution at pH 4. Moreover, after soaking in the buffer solution at pH 9, the patterned hydrogel surfaces

showed highly swollen morphology, which indicates deformed or irregularly patterned structures. However, the change in surface morphology was more significant in the GO-incorporated hydrogel than in the pure copolymer hydrogel surface. The surface image of the GO-incorporated hydrogel shows higher shrinkage at low pH as shown in Figure 4(a). The cross-sectional image in the inset of Figure 4(a) shows that the hydrogel changed into more sticky film. The remarkable changes in the GO-incorporated composite hydrogel surface can be attributed to the added GO in the hydrogel. The additional GO facilitated good interfacial interactions among the GOs in the composite hydrogel surface in the aqueous solution.

The surface morphology of the composite hydrogel surface is sensitive to the pH of the buffer solution; however, the reversibility of the surface pattern obtained by repeated changes in different pH solutions for the same gel is more important. The reversibility of the pattern morphology and the hydrophobic interactions induced by environmental pH change is crucial for the use of hydrogel as a biomimetic smart material. The SEM images shown in Figure 4(c) indicate the pH-dependent reversibility of the surface morphology of the composite hydrogel. The left and right images show the hydrogel film obtained by soaking alternately in pH 4 and 9 buffer solutions. The left image shows the hydrogel obtained at pH 4, whereas the right image shows the

hydrogel obtained at pH 9 during the repeated process. The observed pattern was not completely similar to the patterns obtained in the buffer solutions of pH 4 or 9 under separate conditions, as shown in Figure 4(b). However, the pattern was similarity to those recovered by alternate soaking in different pH solutions.

3.2. Adsorption and desorption of Ag nanoparticles on patterned hydrogel surfaces

Figure 5(a) shows the adsorptivity of the four hydrogel surfaces obtained in separate beakers containing the same concentration (approximately 0.01 M) of Ag nanoparticles in pH 4 buffer solution at 45 °C. The change in the concentration of Ag nanoparticles was measured using a flowing UV–vis detector by placing the hydrogel films (1.5 cm×1.5 cm×1.0 mm) into the solution. The wavelength of the absorbance of Ag concentration was determined using a flowing UV–vis detector at 450 nm, which is the characteristic band of Ag nanoparticles.[55, 58] The concentration of Ag nanoparticles in the buffer solutions at pH 4 decreased with time because of the adhesive hydrophobic interactions between the hydrogel surface and Ag nanoparticles at low pH. The highest adsorptivity of the hydrogel surface at pH 4 was obtained in the patterned GO-incorporated hydrogel film. The GO-incorporated flat hydrogel film, patterned hydrogel film without GO incorporation, and flat hydrogel film without GO incorporation are demonstrated in Figure 5(a). Figure 5(a) also shows that the adsorption rate (i.e., slope)

and the maximum adsorption amount (i.e., absorbance at infinite time) were highest in the patterned GO-incorporated composite hydrogel film among the hydrogel films. In addition, Figure 5(a) shows that the adsorptivity of the GO-incorporated flat hydrogel film and the patterned hydrogel film without GO incorporation was approximately similar. This finding indicates that incorporating GO into the polymer hydrogel and patterning the hydrogel surface with highly ordered structure positively affected the adsorption of nanoparticles on the hydrogel surface at low pH. This result can be attributed to the GO incorporation into the hydrogel that stimulated the changes in the hydrophobic interactions of the hydrogel surface. The remaining carboxyl groups (–COO^-/–COOH) and hydroxyl groups (–O^-/–OH) also provided additional changes even if they were modified to PEG–GO by PEG-amine. The high specific surface area of the patterned morphology of the hydrogel surface also facilitated the adsorption of nanoparticles.

The release rate of the adsorbed Ag nanoparticles at high pH buffer solution was also measured by considering the reversible adsorption–desorption of target nanoparticles on the hydrogel surfaces induced by periodic pH variations. For the release experiment, the four types of hydrogel films were soaked at room temperature in separate beakers containing the same concentration of Ag nanoparticles at pH 4 for

30 min to achieve sufficient adsorption. The concentration of Ag nanoparticles in each beaker was then measured using a UV–Vis spectrometer. Each hydrogel surface adsorbed by Ag nanoparticles was soaked in different beakers containing pH 9 buffer solution without Ag nanoparticles. The concentration of Ag was measured again.

Figure 5(b) shows the results of the release experiment in pH 9 buffer solution at 45 °C. The results indicate that the adsorbed Ag nanoparticles were released from the hydrogel surface because the absorbance (concentration of Ag particles) was gradually increasing with time. Moreover, the rate of release (i.e., slope) was highest in the patterned GO-incorporated composite hydrogel film among the hydrogel films. This result is inconspicuous considering the high adsorptivity of the patterned GO-incorporated hydrogel film at lower pH solution, as shown in Fig. 5(a). The high releasing rate in the patterned GO-incorporated hydrogel film can be attributed to the high escaping rate of Ag nanoparticles from the hydrogel surface. Moreover, the high surface area caused by the patterned structure and the added GO with high surface area can induce the uniform adhesion of Ag nanoparticles on the hydrogel surface with low density during adsorption. The additional ionic repulsion force induced by the functional groups of GO, such as GO–COO^- and GO–O^-, can also accelerate the release of Ag nanoparticles from the GO-incorporated hydrogel surface.

3.3. Adsorption–desorption oscillations of Ag nanoparticles on the patterned GO-incorporated composite hydrogel surface

The adsorption and desorption of Ag nanoparticles on the patterned GO-incorporated hydrogel surface was significantly affected by the pH of the buffer solutions, as shown in Figure 5. The occurrence of the reversible adsorption–desorption of nanoparticles on the hydrogel surface under periodic pH variation were confirmed.

To determine the pH-induced reversible adsorption–desorption oscillations of Ag nanoparticles on the patterned GO-incorporated hydrogel surface, we used the pH-oscillatory system composed of Na_2SO_3–$NaBrO_3$–$K_4Fe(CN)_6$–H_2SO_4, as suggested by Poros et al.[39] The total volume of the reaction mixture in the pH oscillator was decreased to 25 mL in a 50 mL beaker to maximize the intensity of the adsorption–desorption oscillations. In this arrangement, the ratio of $[Na_2SO_3]_o/[H_2SO_4]_o$ in the gel should be modified to obtain oscillations. The dependence of the pH oscillation pattern on the ratio of $[Na_2SO_3]_o/[H_2SO_4]_o$ is shown in Figure 6. The top parts of Figures 6(a) to 6(d) represented the pH oscillations patterns obtained when the ratio of $[Na_2SO_3]_o/[H_2SO_4]_o$ was varied to 4.8, 5.0, 5.2, and 5.4, respectively.

No pH oscillations were observed when the ratio was lower than 4.8 as shown in Figure 6(a), whereas few oscillations were detected in the solutions at pH 6.5 to pH 4 at the ratios of 5.0 and 5.2, as shown in Figures 6(b) and 6(c), respectively. Long-term oscillations were observed at $[Na_2SO_3]_o/[H_2SO_4]_o = 5.4$, in which the oscillations lasted longer than 200 min, with a period of approximately 12 min, as shown in Figure 6(d). However, the ratio further increased, resulting in shortening the duration of the pH oscillations.

The adsorption–desorption oscillations of Ag nanoparticles on the GO-incorporated hydrogel surface induced by the pH-oscillatory reaction system are shown in the bottom parts of Figure 6. To observe heterogeneous oscillations, the hydrogel surface was immersed into the pH-oscillatory reaction mixture, in which 0.01 M Ag nanoparticles (10 nm) were dispersed. The aggregation of Ag particles, which could inhibit the adsorption–desorption oscillations, was not observed in the system. The bottom parts of Figures 6(a) to 6(d) show the results of the adsorption–desorption oscillations of Ag nanoparticles on the GO-incorporated composite hydrogel surface induced by the pH-oscillatory system under the conditions given in the corresponding upper parts. As shown in the bottom parts of Figure 6(a), adsorption–desorption oscillations were not observed when pH oscillations were not obtained. Adsorption–

desorption oscillations appeared when pH oscillations were obtained for specific periods, as shown in Figures 6(b) and 6(c). Figure 6(d) shows a typical adsorption–desorption oscillations induced by the pH-oscillatory system. In this figure, the adsorption–desorption oscillations lasted significantly longer and exhibited similar patterns with the pH oscillations shown in Figure 6(d). The periods of the two types of oscillations, namely, λ_1 and λ_2, were 12 and 14 min, respectively. The induction time (I_2) in the adsorption–desorption oscillations was longer than that in the homogeneous pH oscillations (I_1). The time gap in the period and the longer induction time was due to the delay of the adsorption–desorption oscillations in the heterogeneous reaction to the pH oscillations in the homogeneous system. The results in Figure 6 prove that the observed patterns of the adsorption–desorption oscillations are similar to the pH oscillations, in spite of a small difference in the oscillation period and induction time.

To exclude the possibility that the adsorption–desorption oscillations shown in the bottom parts of Figure 6 were caused by the ferrocyanide/ferrocyanide redox couple used in the pH-oscillator, we performed a blind experiment without GO incorporation and Ag nanoparticles in the pH oscillation solution. No change in absorbance in the pH-oscillatory mixture determined with a UV-Vis spectrometer (Model No. UVIKON xs, 99-90289) at λ = 450 nm was observed. These results indicate that the absorbance

determined with a flowing UV detector (Figure 6) can be attributed to the change in concentration of Ag nanoparticles.

4. Conclusions

A novel and more efficient pH-responsive hydrogel was prepared by incorporating GO into PMAA copolymerized with PEG hydrogel. A regularly-patterned film was prepared with a honeycomb-patterned PS film as template to increase responsivity and compared with un-patterned flat film. The surface morphology and adsorption–desorption interactions of the patterned hydrogel surface were significantly altered by pH change. The surface became hydrophobic under lower pH and hydrophilic under higher pH condition. In addition to the adsorptivity at low pH, the desorption rate at high pH buffer solution was also relatively high in the patterned and composite hydrogels with GO, respectively. A pH oscillator in a closed reaction system composed of BrO_3^-–$Fe(CN)_6^{4-}$–SO_3^{2-} was used to generate periodic adsorption–desorption of Ag nanoparticles on the composite hydrogel surfaces. The adsorption–desorption oscillations were approximately synchronized with the pattern of pH oscillations. These results can be interpreted by the increased responsivity caused by the incorporated GO in the hydrogel. The increased responsivity can be attributed to the increased surface area and abundant hydrophilic groups on the GO surface, as well as to the patterning of

the hydrogel surface morphology, which increased the surface area for adsorption–desorption. The heterogeneous oscillations observed in this study indicate that the adsorption–desorption interactions were reversibly changed on the patterned pH-responsive hydrogel surface. This finding is similar to various natural biological systems.

ACKNOWLEDGEMENTS

This research was supported by the National Research Foundation of Korea, funded by the Ministry of Education, Science, and Technology (2013-R1A1A2A100062399), and partially supported by the 2014 Korea–China Collaboration research fund (2013K2A2A000527). M. Orban is grateful for the grant from the Hungarian Academy of Sciences, OTKA 100891. Huh greatly thanks to Prof. Kozo Kuchitsu for his helpful discussions and comments for the improvement of the paper.

Notes and references

[a] Department of Chemistry and Nanoscience and Engineering, Institute of Basic Science, Inje University, Obang 607, Gimhae City, South Korea

[b] Department of Analytical Chemistry, L. Eötvös University, H-1518 Budapest 112, P.O. Box 32, Hungary

[c] Technical Institute of Physics and Chemistry, Chinese Academy of Sciences, Zhongguancun North First Street 2,100190 Beijing, PR China

1. Z. Ding, G. Chen and A. S. Hoffman, *J. Biomed. Mater. Res.*, 1998, **39**, 498–505.

2. P. S. Stayton, T. Shimoboji and C. Long, *Nature*, 1995, **378,** 472–47423.

3. Z. Ding, G. Chen and A. S. Hoffman, *J. Biomed. Mater. Res.*, 1998, **9**, 498–505.

4. P. S. Stayton, T. Shimoboji, C. Long, A. Chilkoti, G. H. Chen, J. M. Harris and A. S. Hoffman, *Nature*, 1995, **378**, 472–474.

5. Z. Hu, Y. Chen, C. Wang, Y. Zheng and Y. Li, *Nature*, 1998, **393**, 149–152.

6. J. Hrouz, M. Ilavský, K. Ulbrich and J. Kopeček, *J. Euro. Poly.*, 1981, **17**, 361–366.

7. I. C. Kwon, Y.H. Bae and S. W. Kim, *Nature*, 1991, **354**, 291–293.

8. E. Kokufuta and T. Tanaka, *Macromolecules*, 1991, **24**, 1605–1607.

9. A. Suzuki and T. Tanaka, *Nature*, 1990, **346**, 345–347.

10. C. B. Packhaeuser, J. Schnieders, C. G. Oster and T. Kissel, *Eur. J. Pharm. Biopharm.,* 2004, **58**, 445–455.

11. A. Hatefi and B. Amsden, *J. Control. Release*, 2002, **80**, 9–28.

12. B. Jeong, Y. H. Bae and S. W. Kim, *Nature*, 1997, **388**, 860–862.

13. B. Jeong and A. Gutowska, *Trends Biotechnol.*, 2002, **20**, 305–311.

14. Z. L. Wu, M. Moshe, J. Greener, H. Therien-Aubin, Z. Nie, E. Sharon and E. Kumacheva, *Nature Commun.,* 2013, **4**, 1586.

15. C. Keplinger, J. Y. Sun, C. C. Foo and P. Rothemund, *Science*, 2013, **341**, 984-987.

16. Y. Qiu and K. Park, *Adv. Drug Delivery*, 2001, **53**, 321–339.

17. T. Tanaka and D. J. Fillmore, *J. Chem. Phys.*, 1979, **70**, 1214–1218.

18. D. Kuckling, C. D. Vo and S. E. Wohlrab, *Langmuir*, 2002, **18**, 4263–4269.

19. M. E. Harmon, D. Kuckling and C. W. Frank, *Macromolecules*, 2003, **36**, 162–172.

20. M. E. Harmon, D. Kucking and C. W. Frank, *Langmuir*, 2003, **19**, 10660–10665.

21. M. J. Serpe, C. D. Jones and L. A. Lyon*, Langmuir*, 2003, **19**, 8759–8764.

22. D. Kuckling, C. D. Vo, H. J. P. Adler, A. Volkel and H. Colfen, *Macromolecules*, 2006, **39**, 1585–1591.

23. J. Hegewald, T. Schmidt, K. J. Eichhorn, K. Kretschmer, D. Kuckling and K. F. Arndt, *Langmuir*, 2006, **22**, 5152–5159.

24. S. Y. Yu, J. H. Hu, X. Y. Pan and P. Yao, M, Jiang, *Langmuir*, 2006, **22**, 2754–2759.

25. Y. Akiyama, T. Fujiwara, S. I. Takeda, Y. Izumi and S. Nishijima, *Colloid Polym. Sci.*, 2007, **285**, 801–807.

26. P. W. Beines, I. Klosterkamp, B. Menges, U. Jonas and W. Knoll, *Langmuir*, 2007, **23**, 2231–2238.

27. O. Pitois and B. Francois, *Colloid Polym. Sci.*, 1999, **277**, 574–578.

28. H. Yabu and M. Shimomura, *Polymer Journal*, 2008, **40(6)**, 534–537.

29. H. Yabu, Y. Hirai and M. Shimomura, *Langmuir*, 2006, **22(23)**, 9760-9764.

30. H. Yabu, M. Shimomura, *Langmuir*, 2005, **21(5)**, 1709-1711.

31. H. Yabu, R. Jia, Y. Matsuo, K. Ijiro, S. Yamamoto, F. Nishino, T. Takaki, M. Kuwahara and M. Shimomura, *Adv. Mater.*, 2008, **20**, 4200–4204.

32. R. Yoshida, *Adv. Mater.*, 2010, **22**, 3463–3483.

33. R. Yoshida, T. Yamaguchi and H. Ichijo, *Mater. Sci. Eng.*, 1996, **4**, 107–113.

34. S. A. Giannos, S. M. Dinh and B. Berner, *J. Pharm. Sci.*, 1995,**84**, 539–543.

35. G. Rabai and I. R. Epstein, *J. Am. Chem. Soc.*, 1992, **114 (4)**, 1529–1530.

36. G. Rábai and I. Hanazaki, *J. Phys. Chem.*, 1996, **100 (25)**, 10615–10619.

37. G. Rabai and I. Hanazaki, *J. Phys. Chem.*, 1994, **98 (10)**, 2592–2594.

38. G. Rábai, *Phys. Chem. Chem. Phys.*, 2011, **13**, 13604-13606.

39. E. Poros, V. Horvath, K. Kurin-Csörgei, I. R. Epstein and M. Orbán, *J. Am. Chem. Soc*., 2011, **133**, 7174-7179.

40. L. Wang, J. Ren and M. Yao, *Chinese J. Polym. Sci.*, in press.

41. C. Bilici, S. Karayel and T. T. Demir, O. Okay, *J. Appl. Polym. Sci.*, 2010, **118(5)**, 2981–2988.

42. J. Liang, Y. Huang, L. Zhang, Y. Wang, Y. Ma, T. Guo and Y. Chen, *Adv. Funct. Mater.*, 2009, **19**, 1–6.

43. H. Kim, A. A. Abdala and C. W. Macosko, *Macromolecules*, 2010, **43**, 6515–6530.

44. C. W. Sengupta, M. Bhattacharya, S. Bandyopadhyay and A. K. Bhowmick, *Prog. Polym. Sci.*, 2011, **36**, 638–670.

45. H. Bai, C. Li, X. Wang and G. Shi, *Chem. Commun.*, 2010, **46**, 2376–2378.

46. V. Sridhar and I. Oh, *J. Colloid Interface Sci.*, 2010, **348**, 384–387.

47. C. W. Lo, D. Zhu and H. Jiang, *Soft Matter.*, 2011, **7**, 5604–5609.

48. S. Sun and P. Wu, *J. Mater. Chem.*, 2011, **21**, 4095–4097.

49. A. K. Geim and K. S. Novoselov, *Nature Mater.*, 2007, **6**, 183–191.

50. A. A. Balandin, S. Ghosh, W. Z. Bao, I. Calizo, D. Teweldebrhan, F. Miao and C. N. Lau, *Nano Lett.*, 2008, **8**, 902–907.

51. C. Lee, X. D. Wei, J. W. Kysar and J. Hone, *Science*, 2008, **321**, 385–388.

52. M. D. Stoller, S. J. Park, Y. W. Zhu, J. H. An and R. S. Ruoff, *Nano Lett.*, 2008, **8**, 3498–3502.

53. W. S. Hummers and R. E. Offeman, *J. Am. Chem. Soc.,* 1958, **80**, 1339–1339.

54. X. Sun, Z. Liu, K. Welsher, J. T. Robinson, A. Goodwin, S. Zaric and H. Dai, *Nano Res.*, 2008, **1**, 203 – 212.

55. J. K. Kim, K. I. Kim, C. Basavaraja, G. Rábai and D. S. Huh, *J. Phys. Chem. B*,

2013, **117**, 6294–303.

56. J. Roncali, *J. Mater. Chem*, 1997, **7**, 2307–2321.

57. B. S. Kim, W. J. Kim, Y. D. Kim and D. S. Huh, *Bull. Korean Chem. Soc.*, 2011, **32(12)**, 4221–4225.

58. A. Šileikaite, I. Prosycevas, J. Puiso, A. Juraitis and A. Guobiene, *Mater. Science*, 2006, **12**, 287–291.

Table of Contents

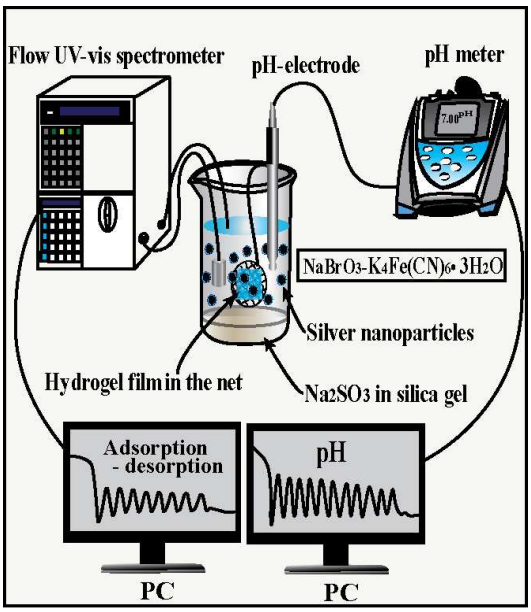

[Figure Captions]

Figure 1. Schematic diagram for the fabrication of patterned GO-incorporated composite hydrogel film using the honeycomb-patterned PS film as a template.

Figure 2. Experimental scheme for the simultaneous detection of pH and adsorption–desorption oscillations induced by the pH oscillator in a closed system.

Figure 3. Typical SEM images of patterned hydrogel film. (a) GO was not incorporated in the film, and (b) GO was incorporated in the composite hydrogel film. The left, right, and bottom images show the surface, cross-sectional image, and SEM-EDS analysis results, respectively. (c) Typical SEM image of the honeycomb-patterned PS film used as a template.

Figure 4. Typical SEM images showing the morphology change of the patterned hydrogel surface by pH variations. (a) In the film without GO incorporation, (b) in the composite hydrogel film with GO incorporation. (c) SEM images showing the pH-dependent reversibility of the surface morphology of the GO-incorporated composite hydrogel obtained by alternate soaking of the hydrogel film in the buffer solutions of pH 4 and 9.

Figure 5. (a) Adsorptivity of Ag nanoparticles on the four types of hydrogel film at pH 4 buffer solutions. (b) Release of Ag nanoparticles with time on the four types of

hydrogel film at pH 9 buffer solutions.

Figure 6. Dependence of the pH oscillation pattern (Top view) and the adsorption-desorption oscillations pattern induced by the pH oscillations (Bottom view) on the ratio of $[Na_2SO_3]_o/[H_2SO_4]_o$ in the gel used in the pH oscillatory system of Na_2SO_3–$NaBrO_3$–$K_4Fe(CN)_6$–H_2SO_4. The ratio $[Na_2SO_3]_o/[H_2SO_4]_o$ in the gel preparation corresponds to (a) 4.8, (b) 5.0, (c) 5.2, and (d) 5.4 at $NaBrO_3$ = 0.09 M, $K_4Fe(CN)_6$ = 0.015 M, T = 45 °C, and 200 rpm stirring rate.